Organic & Biomolecular Chemistry

Accepted Manuscript

ROYAL SOCIETY OF CHEMISTRY

www.rsc.org/obc

Cite this: DOI: 10.1039/c0xx00000x

www.rsc.org/xxxxxx

ARTICLE TYPE

Mechanism and Regioselectivity of Gold (I) or Platinum (II) Catalyzed Intramolecular Hydroarylation to Pyrrolopyridinones and Pyrroloazepinones

Ran Fang Xiaoxiao Wei and Lizi Yang**

Received (in XXX, XXX) Xth XXXXXXXXX 20XX, Accepted Xth XXXXXXXXX 20XX
DOI: 10.1039/b000000x

We report here the theoretical analysis of the mechanism and regioselectivity of gold (I) or platinum (II) catalyzed intramolecular hydroarylation to pyrrolopyridinones and pyrroloazepinones. $AuPH_3^+$ and $PtCl_2$ have been considered to account for some experimental observations. Our calculation results indicate that in the case of cationic gold the nucleophilic attack of the pyrrole on the activated alkyne occurs in an *exo-dig* fashion generating six-membered intermediate, which upon deprotonation and protodeauration forms pyrrolopyridinone. When platinum is used, an *endo-dig* fashion were located to which generate seven-membered intermediate. After deprotonation and protodeplatination pyrroloazepinone is formed. Whether for *exo-dig* (gold (I)) or *endo-dig* (platinum (II)) cyclization, a [1, 2]-migration would not be needed.

Introduction

Through the years, multicomponent reactions (MCRs) have received increasing attention due to their simplicity, efficiency, atom economy, shortened reaction times, and diversity oriented synthesis. The combination of MCRs with transition-metal-catalysis gives access to complex molecules in few steps as compared to traditional multistep processes. [1] They have played important roles in modern synthetic organic chemistry including drug-discovery research.[2] Over the past decade, organic chemists have witnessed a significant advance in the π-acidic transition metal-catalyzed cyclization of unsaturated precursors for the synthesis of carbo and heterocycles,[3] and new methodologies based on platinum and gold catalysis have grown into a major field of experimental [4] as well as theoretical research.[5,6] For example, a mechanistically interesting platinum-catalyzed intramolecular cyclization of alkynes on the pyrrole and the indole core have been reported by Beller and co-workers.[7] A post-Ugi gold(I)-catalyzed intramolecular hydroarylation approach to the synthesis of indoloazocines [8] and spiroindolines [9] also has been reported by Van der Eycken, and co-workers. It has been reported that if not done intramolecularly, pyrroles do not react selectively in gold catalysis. [10] Recently, Van der Eycken, and co-workers have developed a diversity-oriented regioselective intramolecular hydroarylation for the synthesis of pyrrolopyridinones and pyrroloazepinones employing gold(I)- and platinum(II)-catalysis respectively (**Scheme 1**). [11] According to the experimental results, two general mechanisms were postulated to explain the formation of pyrrolopyridinones and pyrroloazepinones. As depicted in the Scheme 2, Coordination of the metal with the alkyne generates intermediate **A**. In the case of cationic gold the nucleophilic attack of the pyrrole on the activated alkyne occurs in an exo-dig fashion generating intermediate **B**. Also, this intermediate has been reported previously as an important one in gold catalysis. [12] This is followed by a [1, 2]-shift to furnish intermediate **C**, which upon deprotonation and protodeauration forms pyrrolopyridinone **D**. When platinum is used, the nucleophilic attack of the pyrrole on the activated alkyne occurs in an endo-dig fashion generating intermediate **A**. After [1, 2]-shift, deprotonation and protodeplatination pyrroloazepinone **G** is formed.

To our knowledge, there are no detailed theoretical studies available in the literature for the novel gold (I) or platinum (II) catalyzed transformation reported by Van der Eycken, and co-workers. [11] Here, we present a detailed density functional theory (DFT) computational investigation of the mechanism and regioselectivity of the gold (I) or platinum(II) catalyzed intramolecular hydroarylation for the synthesis of pyrrolopyridinones and pyrroloazepinones based on the experimental evidence reported by Van der Eycken, and co-workers. [11] The present DFT study located the transition states for the reactions of interest and performed a vibrational analysis at these stationary points. From the results presented here, we hope to learn more about the factors that control the activation barriers of this important reaction and also further investigate the effects of solvent on the thermodynamic and kinetic properties of these reactions.

Computational Methods

All calculations were carried out with the Gaussian 09 programs.[13] The geometries of all the species were fully optimized by using density functional theory (DFT)[14] of the M06-2X method[15]with the 6-31G(d, p) basis set for all atoms except for Au and Pt, which the small-core Los Alamos (LANL2TZ(f)) pseudopotentials and basis sets that include the Dunning-Huzinaga full TZ and Los Alamos ECPs plus TZ have

been employed with an extra f polarization function.[16] This computational method was successfully applied in the mechanistic studies for a variety of chemical applications.[17].Vibrational frequency calculations done at the M06-2X /6-31G (d, p) level of theory were used to characterize all of the stationary points as either minima (the number of imaginary frequencies (NIMAG=0) or transition states (NIMAG=1)). The relative energies are, thus, corrected for the vibrational zero-point energies (ZPE, not scaled). In several significant cases, intrinsic reaction coordinate (IRC) [18] calculations were performed to unambiguously connect the transition states with the reactants and the products. The solvent effect was taken into account by M06-2X/6-311++G (d, p) single-point calculation with integral equation formalism polarizable continuum model (IEFPCM) in trichloromethane (ε = 4.71). The radii and nonelectrostatic terms were taken from Truhlar and co-workers' universal solvation model (SMD).[19]

Results and Discussion

Energy profiles for reaction pathways of *exo*-dig cyclization and *endo*-dig cyclization are shown in Figures 1[20]. The optimized geometries for the reactants, intermediates, transition states and products of the reactions are depicted schematically in Figure 2 along with selected key geometry parameters (e.g. bond lengths). Their relative energies and free energies in the gas and solution phases, together with the activation barriers corresponding to the relevant transition structures, are shown in Table 1. Unless otherwise noted, the relative free energies discussed in subsequent sections refer to the value in trichloromethane solvent. The detailed structural parameters and energies for the structures determined here are collected in the Supporting Information. To keep the computational cost low, gold's ligand $[AuPPh_3]^+$ replaced with $[AuPH_3]^+$. In the systems studied here, $[AuPH_3]^+$ is a model for $[AuPPh_3]^+$ because the steric effects are minimal due to the fact that the number of ligands around the gold metal center is small (vide infra). In addition, there are many previous works employing $[AuPH_3]^+$ as a model for the catalytically active species $[AuPPh_3]^+$.[21]

3.1 Computational Results for the Au (I)-Catalyzed

The energy profile for pathway **a** and **b** is represented in Figure 1. The structures of the various critical points located on the potential surface along with the values of the most relevant geometry parameters are shown in Figure 2. Generally, the C-C triple bond functional group is characterized by two orthogonal π-bonds, high in energy that easily interacts with the *d* orbitals in transition metals (electrophiles). At the same time, the LUMO in alkynes is low in energy, which allows the attack of strong nucleophiles.[22] From the energy profile it is evident that the first step of pathway **a** indeed involves a preliminary intermediate **1-Au** stabilized by the coordination of the Au atom to the oxygen atom and the π-bond of the alkyne moiety. If we consider $[AuPH_3]^+$ as the "active" species of the catalyst, **1-Au** forms without any barrier and is 43.9 kcal/mol lower in energy than the reactants. In **1**, the lengths of the two Au-C bonds are 3.761 and 3.219 Å and the distance of Au-O is 2.089 Å. These values for bond distance indicate that the major coordination reaction occurs between the gold and oxygen atom rather than π-bond of the alkyne. This fact also can be draw from the orbital interactions of LUMO for **1-Au** (Figure 3). the LUMO for structures **1-Au** describe the orbital overlap between the *p*-orbital of oxygen atom and the d_z^2 orbital of gold atom. Once in **1-Au**, the coordination of the triple bond and oxygen atom with the gold atom enhances the electrophilicity of the triple bond that induces a cyclization of the C^3 onto the triple bond (C^2). A new and stable intermediate **1a** is formed through five-membered **TSa1**. Inspection of Figure 3 shows that the gold atom is completely connected with the C^1 atom of the alkyne (the bond distance Au-C^4 is 2.216 Å) in **TSa1**. Furthermore, the bonds of the C^2-C^3 change from 2.796 to 2.358 Å. Table 1 shows that the energy of activation for this step is calculated to be 10.1 kcal/mol for **TSa1** and the energy of reaction for the **1a** intermediates is -12.9 kcal/mol with respect to **1-Au**. In **1a**, it is evident that the C^1-C^2 triple bond completes its change from a triple bond to a double bond (1.346 Å) and the new bond of C^2-C^3 also becomes completely formed and is now 1.536Å. The subsequent step for [1, 2] shift would be induce the **2a** through **TSa2**. In **TSa2**, the breaking C^2-C^3 bond is 1.745 Å and the forming C^2-C^4 bond is 1.687 Å. The activation free energy of the second step was 19.9 kcal/mol, and the formation of **2a** is an endothermic process (the free energy of reaction for the **2a** was 7.8 kcal/mol with respect to **1a**). A higher activation free energy found for this step indicates that this step is the rate-determining one. Apart from pyrrole ring attacking the alkyne through C^3, this would be the possibility of the pyrrole ring attacking the alkyne through C^4, instead of carbon C^3.[23] This way, a [1, 2]-migration would not be needed. Inspection of Figure 2 shows that the bond distance of C^2-C^4 is 2.157 Å in **TSa3**. The activation free energy of this step was 16.4 kcal/mol, and the formation of **2a** is an exothermic process (the free energy of reaction for the **2a** was -5.1 kcal/mol with respect to **1-Au**). The next step for migration of the hydrogen atom from C^4 to O^1 (**TSa4**) results in the formation of new oxonium ion intermediates **3a** that are -6.7 kcal/mol lower in energy than the reactants. Table 1 shows that this exothermic hydrogen atom migration step proceeds with a lower activation energy (9.9 kcal/mol). The oxonium ion intermediates **3a** would be form the final product (**4a**) and regenerate the catalyst via a second hydrogen atom migration from O^1 to C^1 (transition states **TSa5**). The barriers for this step were 8.5 kcal/mol and were exothermic by -30.7 kcal/mol. The entire catalytic processes are exothermic by -37.9 and -41.5 kcal/mol lower than the starting reactants.

Apart from 5-*exo*-dig cyclization, the attack between the C^3 and the triple bond (C^1) would give rise to another possible reaction pathway in **1-Au.** Examination of Figure 1 shows that the first step for pathway **b** also involves a preliminary intermediate **1-Au**. Cyclization of the C^3 onto the triple bond (C^1) would give a new and stable structure **1b** through a six-membered ring transition structure **TSb1.** In **TSb1**, nucleophilic attack of C^4 on the C^2 leads to the formation of C^2-C^3 bond and the distance of C^2-C^3 in **TSb1** was 1.961 Å. Table 1 showed that the free energy of activation for this step was calculated to be 26.6 kcal/mol for **TSb1** and the free energy of reaction for the **1b** intermediates was -14.2 kcal/mol with respect to **1-Au**. This step also is the rate-determining one for the whole catalytic process. The higher barriers found for **TSb1** than those of **TSa1** can be mainly attributed to the following reasons. Firstly, the NBO charges for the C^1, C^2 and C^3 atoms are -0.130, 0.106 and 0.217 au for **1-Au** , respectively. A positive charge found for C^2 atom makes the

nucleophilic attack of O on the positively charged C^2 more feasible than on C^1 atom. Secondly, the calculation results for orbital interactions of LUMO for **TSa1** and **TSb1** were shown in Figure 3. As we can see from Figure 3, the new formly C^2-C^3 bond attributed to the orbital interactions between $\pi^*(C^1\text{-}C^2)$ and π (C^3-C^4). However, the orbital interactions between $\pi^*(C^1\text{-}C^2)$ and π^* (C^3-C^4) should be responsible for the new formly C^1-C^3 bond for **TSb1**. These differents between orbital interactions cause the nucleophilic attack of C^3 on C^2 more feasible than on C^1 atom. Just as exhibited by the structure of **1a**, the C^1-C^3 bond in **1b** also becomes completely formed. Now is 1.538 Å. Furthermore, the C^1-C^2 bond also accomplished the conversion of triple bond to double bond and now the bond distance was 1.344 Å. Subsequent step for [1, 2] shift would be generate seven carbocation intermediate **2b**. Figure 2 shows that the C^1-C^3 bond was 1.772 Å in **TSb2**. Furthermore, the new forming C^1-C^4 bond is 1.748 Å. The activation free energy of this step is 20.8 kcal/mol, and the formation of **2b** is an endothermic process (the free energy of reaction for the **2b** was 7.2 kcal/mol with respect to **1b**). Just as pathway **a**, this would be another possibility of the pyrrole ring attacking the alkyne through C^4, instead of carbon C^3.[23] Figure 2 shows that the bond distance of C^1-C^4 is 2.435 Å in **TSb3**. The activation free energy of this step was 18.5 kcal/mol, and the formation of **2b** is an exothermic process (the free energy of reaction for the **2a** was -7.0 kcal/mol with respect to **1-Au**). Next step generate the oxonium ion intermediates **3b** through hydrogen atom migration from C^4 to O^1 **(TSb4)**. Figure 2 shows that the bonds of C^4-H and O^1-H were 1.264 and 1.529 Å in **TSb4**, respectively. The activation free energy of this step is 7.1 kcal/mol, and the formation of **3b** is an exothermic process (the free energy of reaction for the **3b** was -8.0 kcal/mol with respect to **2b**). In order to generate the final product (**4b**) and regenerate the catalyst, oxonium ion intermediates **3b** undergo the second hydrogen atom migration (O^1 to C^2 **TSb5**). The activation free energy of the second step is 5.4 kcal/mol, and the formation of **4b** is an exothermic process (the free energy of reaction for the **4b** was -34.6 kcal/mol with respect to **1**). According to our calculated results, **TSa3** and **TSb3** would play vital roles in the title reaction. A higher activation energies found for **TSb3** indicate that the formation of product **4b** from **1** via pathway b should be unfavored. In order to further consider the effect of the legend, the reaction pathways **a** for the $Au(PPh_3)^+$ were calculated and the energy profile for this process is represented in Figure S1. Caculation results show that barriers for **TSa1-Ph**, **TSa2-Ph**, **TSa3-Ph**, **TSa4-Ph** and **TSa5-Ph** were 13.9, 20.8, 15.3, 12.1 and 8.3 kcal/mol, respectively. A little difference between $Au(PPh_3)^+$ and $AuPH_3^+$ indicate that $[AuPH_3]^+$ is a good model for $[AuPPh_3]^+$ for the systems studied here.

3.2 Computational Results for the Pt (II) -Catalyzed

The energy profile for this process is depicted in Figure 4. The structures of the various critical points located on the potential surface along with the values of the most relevant geometry parameters are presented in Figure 5. Examination of Figure 4 shows that the first step for pathway **c** also involves a preliminary intermediate **1-Pt** stabilized by the coordination of the Pt atom and the π-bond of the alkyne moiety. If we consider $PtCl_2$ as the "active" species of the catalyst, **1-Pt** forms without any barrier and is 48.7 kcal/mol lower in energy than the reactants. The higher complexation energies found for **1-Pt** indicated that the interaction with Pt atom to π-bond of the alkyne is significantly stronger than that for Au atom to the carbonyl oxygen atom. Comparison of the structures of **1-Au** with **1-Pt** reveals that the major coordination reaction occurs between the carbonyl oxygen atom and the gold atom in **1-Au**. However, the major coordination reaction takes place between the terminal CC triple bond and the Pt atom in **1-Pt**. In **1-Pt,** the distance of Pt-O is 3.140 Å and the lengths of the two Pt-C bonds are 2.047 and 2.034 Å. These values for bond distance indicate that a symmetrical coordination reaction between the terminal CC triple bond and the Pt atom was found for **1-Pt**. As we mentioned above, the coordination of the triple bond with the Pt atom in **1-Pt** enhances the electrophilicity of the triple bond which make a cyclization of the C^3 onto the triple bond (C^2) and give a new and stable structure **1c** through a five-membered ring transition structures **TSc1**. Table 2 shows that the free energy of activation for this step is calculated to be 9.2 kcal/mol for **TSc1** and the free energy of reaction for the **1c** intermediates is -33.8 kcal/mol with respect to **1-Pt**. **1c** is then converted to the intermediate 2c via an [1,2]-shift transition structure **TSc2**. In **TSc2**, the C^2-C^3 and C^2-C^4 bonds are 1.563 and 1.882 Å, respectively. The activation free energy of this step was 12.6 kcal/mol, and the formation of **2c** is an endothermic process (the free energy of reaction for the **2c** was 8.5 kcal/mol with respect to **1c**). The relatively lower barriers found for **TSc2** than those of **Tsa2** can mainly be attributed to the following reason. There are only relatively small structural changes (C^2-C^3 bond change from 1.519 to 1.563 Å) from the reactants to the transition states. Thus, not much energy is needed to go from the reactant to the transition states. Also this would be the possibility of the pyrrole ring attacking the alkyne through C^4, instead of carbon C^3.[23] Figure 5 shows that the bond distance of C^2-C^4 is 2.033 Å in **TSc3**. The activation free energy of this step was 10.7 kcal/mol, and the formation of **2c** is an exothermic process (the free energy of reaction for the **2c** was -25.3 kcal/mol with respect to **1-Pt**). Next step for hydrogen atom migration from C^4 to O^1 would be generating the intermediates **3c**. Figure 5 shows that the bonds of C^4-H and O^1-H were 1.298 and 1.487 Å in **TSc4**, respectively. The activation free energy of this step is 13.1 kcal/mol, and the formation of **3c** is an exothermic process (the free energy of reaction for the **3c** was -16.1 kcal/mol with respect to **2c**). The subsequent step for two consecutive migration of the hydrogen atom would be inducing the final product (**5c**) and regeneration of the catalyst. The barriers of 17.5 and 9.5 kcal/mol are required for **TSc5** and **TSc6**, respectively.[24] The whole catalytic processes are exothermic by -40.4 kcal/mol lower than **1-Pt**. The higher barriers found for **TSc5** indicate that this step also was the rate-determining one.

Simlar to gold (I)-catalyzed, the attack between the C^3 and the triple bond (C^1) would give rise to another possible reaction pathway in **1-Pt.** Cyclization of the C^3 onto the triple bond (C^1) would give a new and stable structure **1d** through a six-membered ring transition structure **TSd1.** In **TSd1**, nucleophilic attack of C^3 on the C^1 leads to the formation of C^1-C^3 bond and the distance of C^1-C^3 in **TSd1** was 2.442 Å. Table 2 showed that the free energy of activation for this step was calculated to be 10.5 kcal/mol for **TSd1** and the free energy of reaction for the **1d** intermediates was

-34.1 kcal/mol with respect to **1-Pt**. The C^1-C^3 bond in **1d** becomes completely formed and now is 1.523 Å. Furthermore, the C^1-C^2 bond also accomplished the conversion of triple bond to double bond and now the bond distance was 1.346 Å. Subsequent step would be generate seven-membered intermediate **2d** through **TSd2**. Figure 5 shows that the C^1-C^3 bond changed from 1.523 to 1.575 Å in **TSd2**. Furthermore, the new forming C^1-C^4 bond is 1.834 Å. The activation free energy of this step is 15.9 kcal/mol, and the formation of **2d** is an endothermic process (the free energy of reaction for the **2d** was 8.5 kcal/mol with respect to **1d**). Similar to pahway c, this also would be the possibility of the pyrrole ring attacking the alkyne through C^4, instead of carbon C^3.[23] Inspection of Figure 5 shows that the bond distance of C^1-C^4 is 2.506 Å in **TSd3**. The activation free energy of this step was 14.6 kcal/mol, and the formation of **2d** is an exothermic process (the free energy of reaction for the **2d** was -23.1 kcal/mol with respect to **1-Pt**).Next step generate the oxonium ion intermediates **3d** through hydrogen atom migration from C^4 to O^1 **(TSd4)**. Figure 5 shows that the bonds of C^4-H and O^1-H were 1.264 and 1.529 Å in **TSd4**, respectively. The activation free energy of this step is 5.4 kcal/mol, and the formation of **3d** is an exothermic process (the free energy of reaction for the **3b** was -9.9 kcal/mol with respect to **2d**). In order to generate the final product (**4d**) and regenerate the catalyst (R2), **3d** undergo the second hydrogen atom migration (O^1 to C^1 **TSd5**). The activation free energy of the second step is 12.8 kcal/mol, and the formation of **4d** is an exothermic process (the free energy of reaction for the **4d** was -7.1 kcal/mol with respect to **3d**). According to our calculated results, **TSc5** and **TSd2** would play vital roles in the platinum (II) -Catalyzed reaction. A higher activation energies found for **TSc5** indicate that the formation of product **4c** from **1-Pt** *via* pathway **a** would be unfavored. Our calculated results are in good agreement with the experimental observations. [11]

3.3 *exo-dig* fashion vs *endo-dig* fashion

According to our calculation results, in the case of cationic gold the nucleophilic attack of the pyrrole on the activated alkyne occurs in an *exo-dig* fashion generating six-membered intermediate, which upon deprotonation and protodeauration forms pyrrolopyridinone. When platinum is used, an *endo-dig* fashion were located to which generate seven-membered intermediate. After deprotonation and protodeplatination pyrroloazepinone is formed. In order to further consider the effect of different metal complexes, the reaction mechanism catalyzed by gold (III) has been performed. The calculation results clearly indicate that gold (III) prefer a pathway similar to platinum (II) – Catalyzed. That is to say, the nucleophilic attack of the pyrrole on the activated alkyne occurs in an *endo-dig* fashion generating seven-membered intermediate, which upon deprotonation and protodeplatination forms pyrroloazepinone. [25] As we known, Cationic Au(I) species are superior Lewis acids compared with other Group 11 metals for many transformations, and intuitively it seems that relativistic contraction of the valence s or p orbitals of Au should be responsible, because they should correspond to a relatively low-lying lowest unoccupied molecular orbital (LUMO) and therefore strong Lewis acidity. This conclusion can also be derived from considering the major coordination between the metal and oxygen atom. The major coordination reaction occurs between the carbonyl oxygen atom and the gold atom in **1-Au**. However, the major coordination reaction takes place between the terminal CC triple bond and the Pt atom in **1-Pt**. The strong Lewis acidity of gold (I) might explain why other metal complexes prefer a pathway involved an *endo-dig* fashion.

Conclusions

In summary, this work has provided the detailed theoretical study for the reaction of the gold (I) or platinum (II) catalyzed intramolecular hydroarylation to pyrrolopyridinones and pyrroloazepinones. In the case of cationic gold, our calculation results suggested that the first step of the cycle is the pyrrole ring attacking the alkyne through C^4 via an *exo-dig* fashion generating generating six-membered intermediate, which upon deprotonation and protodeauration produces the observed products and liberate the cationic gold (I) catalyst. A [1, 2]-migration would not be needed. On the other hand, when platinum is used, an *endo-dig* fashion were located to which generate seven-membered intermediate. Also, a [1, 2]-migration would not be needed. After deprotonation and protodeplatination pyrroloazepinone is formed. Whether for *exo-dig* (gold (I)) or *endo-dig* (platinum (II)) cyclization, the first step for pyrrole ring attacking the alkyne through C^4 was the rate-determining one. These calculated results are consistent with the experimental observations of Van der Eycken, and co-workers for the synthesis of pyrrolopyridinones and pyrroloazepinones through gold (I) - and platinum (II)-catalysis respectively. The predictions may be useful as a guide to future synthetic efforts and to problems that merit further study by both theory and experiment.

Notes and references

Key Laboratory of Nonferrous Metals Chemistry and Resources Utilization of Gansu Province and College of Chemistry and Chemical Engineering, Lanzhou University, Lanzhou 730000, P. R. China; E-mail: fangr@lzu.edu.cn, yanglz@lzu.edu.cn

† Electronic Supplementary Information (ESI) available: [details of any supplementary information available should be included here]. See DOI: 10.1039/b000000x/

1 (a) A. Dömling and I. Ugi, *Angew. Chem., Int. Ed.*, 2000, **39**, 3168; (b) A. Dömling, *Chem. Rev.*, 2006, **106**, 17; (c) D. J. Ramón and M. Yus, *Angew. Chem., Int. Ed.*, 2005, **44**, 1602; (d) B. Ganem, *Acc. Chem. Res.*, 2009, **42**, 463; (e) E. Ruijter, R. Scheffelaar and R. V. A. Orru, *Angew. Chem., Int. Ed.*, 2011, **50**, 6234; (f) A. Dömling, W. Wang and K. Wang, *Chem. Rev.*, 2012, **112**, 3083; (g) M. Shiri, *Chem. Rev.*, 2012, **112,** 3508.(h) X. Guo and W. Hu, *Acc. Chem. Res.*, 2013, **46**, 2427.

2 (a) C. Hulme, V. Gore, *Curr. Med. Chem*. 2003, **10**, 51. (b) R. V. A. Orru, M. de Greef, *Synthesis* 2003, 1471. (c) D. J. Ramón, M. Yus, *Angew. Chem., Int. Ed.* 2005, **44**, 1602. (d) B. Ganem, *Acc. Chem. Res.* 2009, **42**, 463. (e) B. B. Toure, D. G. Hall, *Chem. Rev.* 2009, **109**, 4439.

3 (a) A. Fürstner and P. W. Davies, *Angew. Chem., Int. Ed.*, 2007, **46**, 3410; (b) A. Fürstner, *Chem. Soc. Rev.*, 2009, **38**, 3208; (c) A. S. K. Hashmi and M. Rudolph, *Chem. Soc. Rev.*, 2008, **37**, 1766; (d) M. Rudolph and A. S. K. Hashmi, *Chem. Commun.*, 2011, **47**, 6536; (e) M. Rudolph and A. S. K. Hashmi, *Chem. Soc. Rev.*, 2012, **41**, 2448; (f) E. Jiménez-Núñez and A. M. Echavarren, *Chem. Commun.*, 2007, 333; (g) A. M. Echavarren, *Nat. Chem.*, 2009, **1**, 431; (h) A. S. K. Hashmi, W. Yang and F. Rominger, *Angew. Chem., Int. Ed.,* 2011, **50**, 5762; (i) A. Arcadi, *Chem. Rev.*, 2008, **108**, 3266; (j) A. S. K. Hashmi, *Chem. Rev.*, 2007, **107**, 3180; (k) Z. Li, C. Brouwer and C. He, *Chem. Rev.*, 2008, **108**, 3239; (l) D. J. Gorin, B. D. Sherry and F. D. Toste, *Chem. Rev.,* 2008, **108**, 3351; (m) M. Bandini, *Chem. Soc.*

Rev., 2011, **40**, 1358; (n) H. C. Shen, *Tetrahedron*, 2008, **64**, 3885; (o) H. C. Shen, *Tetrahedron*, 2008, **64**, 7847.

4 (a) C. C. J. Loh, J. Badorrek, G. Raabe and D. Enders, *Chem. –Eur. J.*, 2011, **17**, 13409; (b) M.Hoffmann, J.-M. Weibel, P. de Frémont, P. Pale, A. Blanc, *Org. Lett.* 2014, **16**, 908; (c) M. Kumar, J. Jasinski, G. B. Hammond, *Chem.- Eur. J.* 2014, **20**, 3113; (d)G. Cera, P. Crispino, M. Monari and M. Bandini, *Chem. Commun.*, 2011, **47**, 7803; (e) M. M. Hansmann, M. Rudolph, F. Rominger, A. S. K. Hashmi, *Angew. Chem., Int. Ed.* 2013, **52**, 2593. (f) B. Lu, Y. Li, Y. Wang, D. Aue, H. Y. Luo, L. Zhang, *J. Am. Chem. Soc.* 2013, **135**, 8512. (g) W. Rao, M. J. Koh, D. Li, H. Hirao, P. W. H. Chan, *J. Am. Chem. Soc.* 2013, **135**, 7926. (h) B.Lu, Y. Li, Y. Wang, D. Aue, H. Y. Luo, L. Zhang, *J. Am. Chem. Soc.* 2013, **135**, 8512. (i) A. S. K. Hashmi, W. Yang, Y. Yu, M. M. Hansmann, M. Rudolph, F. Rominger, *Angew. Chem., Int. Ed.* 2013, **52**, 1329. (j) A. S. K. Hashmi, *Acc. Chem. Res.* 2014, **47**, 864.(k) D. Kadzimirsz, D. Hildebrandt, K. Merz and G. Dyker *Chem. Commun.*, 2006, 661–662

5 (a) O. N. Faza, C. S. López, A. R. de Lera, *J. Org. Chem.,* 2011, **76**, 3791; (b) E.Tkatchouk, N. P. Mankad, D. Benitez, W. A.Goddard , F. D. Toste, *J. Am. Chem. Soc*., 2011, **133**, 14293; (c) G. Kovács, A. Lledós, G. Ujaque, *Angew. Chem., Int. Ed.*, 2011, **50**, 11147; (d) Y. Xia, G.Huang, *J. Org. Chem.*, 2010, **75***,* 7842; (e) M.Pernpointner , A. S. K. Hashmi, *J. Chem. Theory Comput*., 2009, **5**, 2717; (f) G. Huang, B. Cheng, L. Xu, Y. Li, Y. Xia, *Chem.–Eur. J.*, 2012, **18**, 5401; (g) B. Cheng, G. Huang, L. Xu , Y. Xia *Org. Biomol. Chem*., 2012, **10**, 4417;(h) T. Zhou, L. Xu, and Y. Xia *Org. Lett.* 2013,**15**, 6074(i)R. Döpp, C. Lothschütz, T. Wurm, M. Pernpointner, S. Keller, F. Rominger, A. S. K. Hashmi, *Organometallics*, 2011, **30**, 5894; (i) C. M. Krauter, A. S. K. Hashmi, M. Pernpointner *ChemCatChem* 2010, **2**, 1226.(k) O. N. Faza, R. Á.Rodríguez, C. S. López, *Theor. Chem. Acc.* 2011, **128**, 647.(l) R. Kang, H. Chen, S. Shaik, J. Yao *J. Chem. Theory Comput*., 2011, **7**, 4002

6 For recent theoretical studies of gold or platinum catalyzed -catalyzed reactions, see: (a) R. Fang, C.-Y. Su, C. Zhao, D. L. Phillips, *Organometallics* 2009, **28**, 741. (b) R. Fang, L. Yang, Y. Wang, *Org. Biomol. Chem*. 2011, **9**, 2760.(c) L. Yang, R. Fang *J. Mol. Catal. A,* 2013, **379**, 197,(d) R. Fang, L.Yang *Organometallics* 2012, **31**, 3043(e)R. Fang; L.Yang; Q. Wang *Organometallics*, 2012, **31**, 4020 (f) M. Vilhelmsen, A. S. K. Hashmi *Chem. Eur. J.* 2014, **20**, 1901–1908;(g) G. Klatt, R. Xu, M. Pernpointner, L. Molinari, T. Q. Hung, F. Rominger, A. S. K. Hashmi, H. Köppel *Chem. Eur. J.* 2013, **19**, 3954-3961

7 (a) M. Gruit, D. Michalik, A. Tillack and M. Beller, *Angew. Chem., Int. Ed*., 2009, **48**, 7212; (b) M. Gruit, A. Pews-Davtyan and M. Beller, *Org. Biomol. Chem*., 2011, **9**, 1148

8 S. G. Modha, D. D. Vachhani, J. Jacobs, L. Van Meervelt and E. V. Van der Eycken, *Chem. Commun.*, 2012, **48**, 6550.

9 S. G.Modha, A. Kumar, D. D. Vachhani, J. Jacobs, S. K. Sharma, V. S. Parmar, L. Van Meervelt and E. V. Van der Eycken, *Angew. Chem., Int. Ed.*, 2012, **51**, 9572.

10. A. S. K. Hashmi, R. Salathé, and W. Frey *Eur. J. Org. Chem*. 2007, 1648-1652

11 S. G. Modha, A. Kumar, D. D. Vachhani, S. K. Sharma, V. S. Parmarb and E.V. Van der Eycken *Chem. Commun.*, 2012, **48**, 10916

12 (a)A. S. K. Hashmi, T. Häffner, W. Yang, S. Pankajakshan, S. Schäfer, L. Schultes, F. Rominger, W. Frey *Chem. Eur. J.* 2012, **18**, 10480-10486;(b) A. S. K. Hashmi, W. Yang, F. Rominger *Chem. Eur. J.* 2012, **18**, 6576-6580;(c) A. S. K. Hashmi, W. Yang, F. Rominger *Adv. Synth. Catal*. 2012, **354**, 1273-1279;(d) A. S. K. Hashmi, W. Yang, F. Rominger *Angew. Chem. Int. Ed.* 2011, **50**, 5762–5765

13 M. J. Frisc h, et al ; *Gaussian 09*, revision A.01; Gaussian, Inc.: Wallingford, CT, U.S., 2009.

14 R. G. Parr, W. Yang, *Density-functional Theory of Atoms and Molecules*; Oxford University Press: New York, 1989.

15 Y. Zhao, D. G. Truhlar *Theor. Chem. Acc.* 2008, **120**, 215-241.

16 a) P. J. Hay, W. R. Wadt, *J. Chem. Phys.* 1985, **82**, 270.b) W. R. Wadt, P. J. Hay, *J. Chem. Phys.* 1985, **82**, 284.c) L. E. Roy, P. J. Hay, R. L. Martin, *J. Chem. Theory Comput*. 2008 ,**4**,1029

17 (a) Y. Zhao, D. G.Truhlar, *J. Phys. Chem. Lett.* 2008, **112**, 1095; (b) D. Jacquemin, E. A. Perpète, I. Ciofini, C. Adamo, R. Valero; Y. Zhao, D. Truhlar, *J. Chem. Theory Comput.* 2010, **6**, 2071; (c) Y. Zhao, D. G. Truhlar, *J. Chem. Theory Comput.* 2008, **4**, 1849; (d) Y. Zhao, D. Truhlar, *Acc. Chem. Res*. 2008, **41**, 157.

18 C. Gonzalez, H. B. Schlegel, *J. Phsy. Chem.* 1990, **94**, 5523.

19 A. V. Marenich, C. J. Cramer, D. G. Truhlar, *J. Phys. Chem. B* 2009, **113**, 6378.

20 S. Kozuch, S. Shaik., *Acc. Chem. Res*. 2011, **44**, 101.

21 (a) R. X. Zhu, D. J. Zhang, J. X. Guo, J. L.Mu, C. G. Duan, C. B. Liu, *J. Phys. Chem. A* 2010, **114**, 4689. (b) G. Kovács, G.Ujaque, A. Lledós, *J. Am. Chem. Soc.* 2008, **130**, 853. (c) A. G. Pérez, C. S. López, J. Marco-Contelles, O. N. Faza, E. Soriano, A. R. D. Lera, *J. Org. Chem.* 2009, **74**, 2982.(d) T. Fan, X. Chen; J. Sun; Z. Lin *Organometallics* 2012, **31**, 4221.

22 M.García-Mota, N. Cabello, F. Maseras, A. M.Echavarren, J. Pérez-Ramírez, N. Lopez, *ChemPhysChem* 2008, **9**, 1624.

23 R. Sanz, D. Miguel, M. Gohain, P. García-García, M. A. Fernández-Rodríguez, A. González-Pérez, O. Nieto-Faza, Á. R. de Lera, Félix Rodríguez *Chem. Eur. J.* 2010, **16**, 9818.

24 As suggested by a reviewer, another possibility would be a direct migration of the proton to the double bond from 2c to 4c, without the intermediacy of the carbonyl group. However, the activation free energy of direct migration of the proton to the double bond is 19.9 kcal/mol.

25 Caculation results including energy profiles and relative free energies and activation free energies in gas phase and in solution for $AuCl_3$ are collected in the Supporting Information (See Figure S2 and Table S2).

Cite this: DOI: 10.1039/c0xx00000x

www.rsc.org/xxxxxx

ARTICLE TYPE

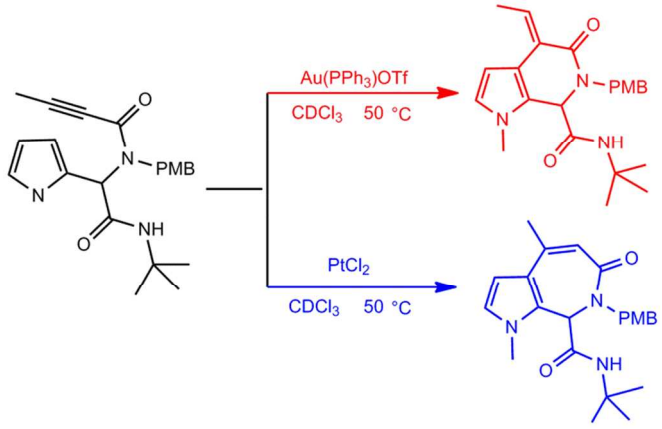

Scheme 1

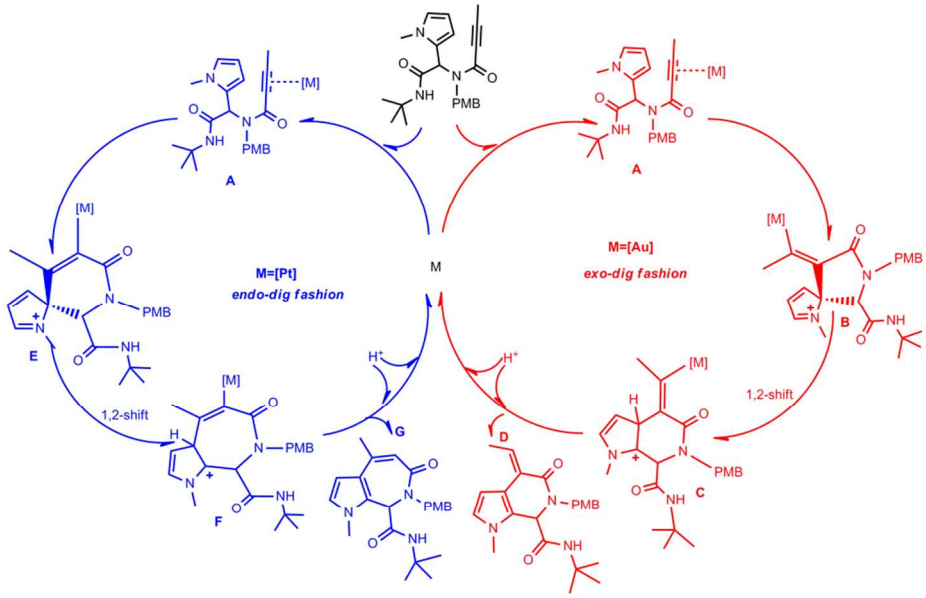

Scheme 2 Two plausible mechanisms for the formation of pyrrolopyridinones and pyrroloazepinones.

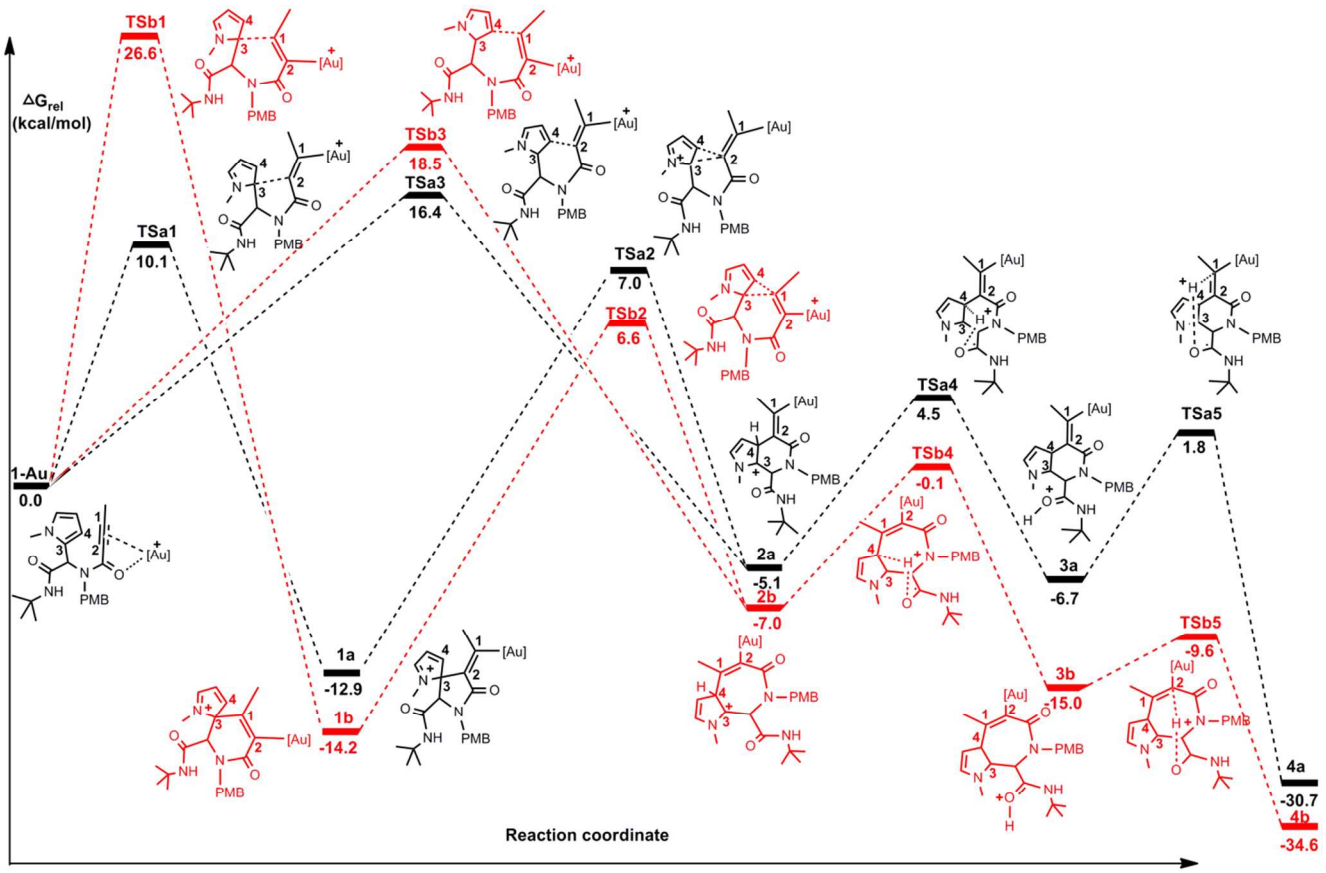

Figure 1. Energy profiles for path **a** and **b**; the relative energies are given in kcal/mol.

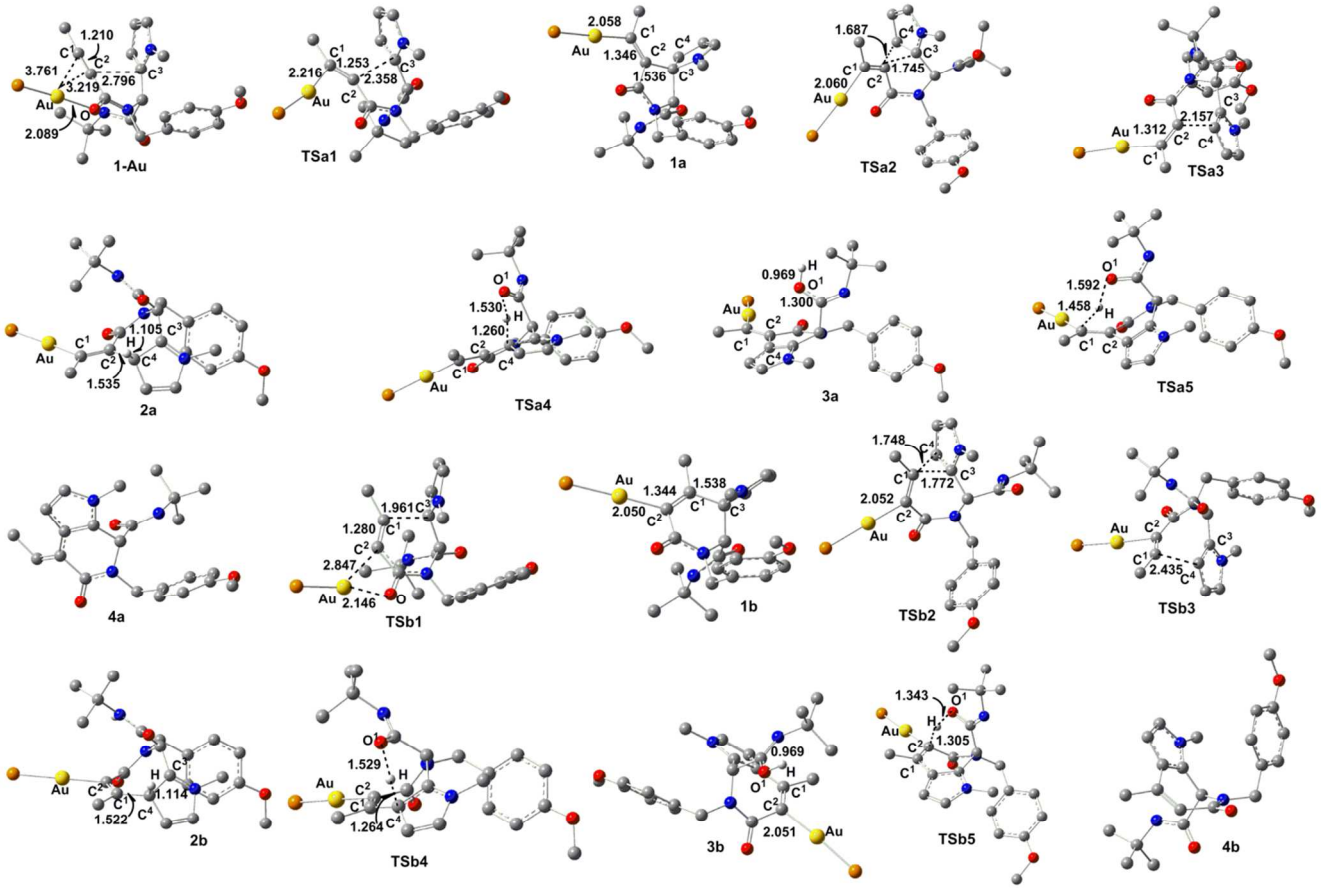

Figure 2 Optimized structures for path **a** and **b** shown in Figure 1, with selected structural parameters (bond lengths in Å).

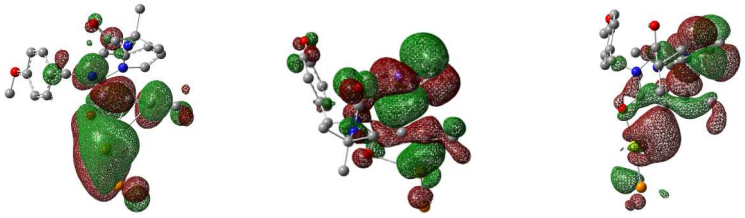

LUMO (**1-Au**) LUMO (**TSa1**) LUMO (**TSb1**)

Figure 3. The orbital interactions for LUMO for structures of **1-Au**, **TSa1** and **TSb1.**

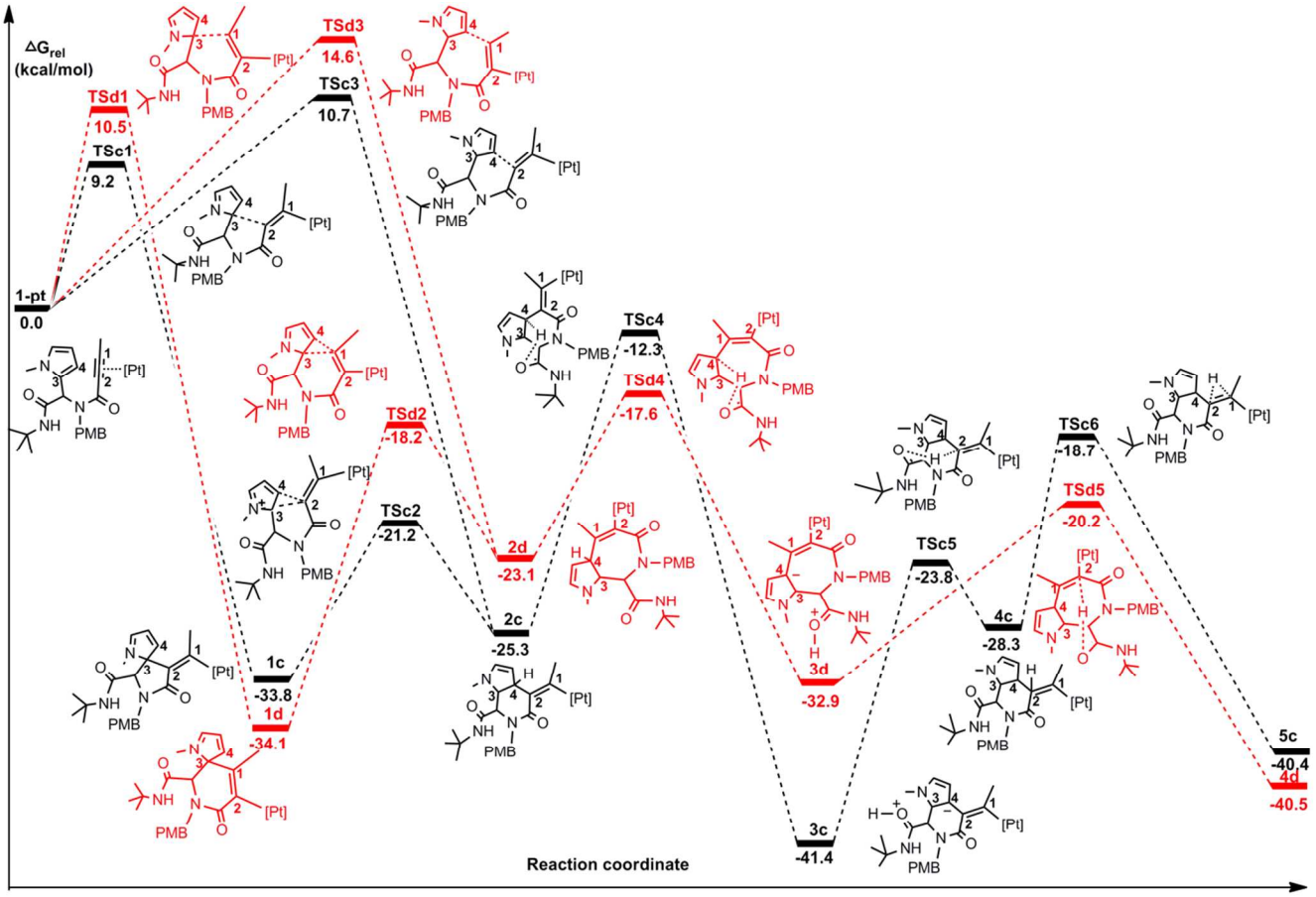

Figure 4. Energy profiles for path **c** and **d**; the relative energies are given in kcal/mol.

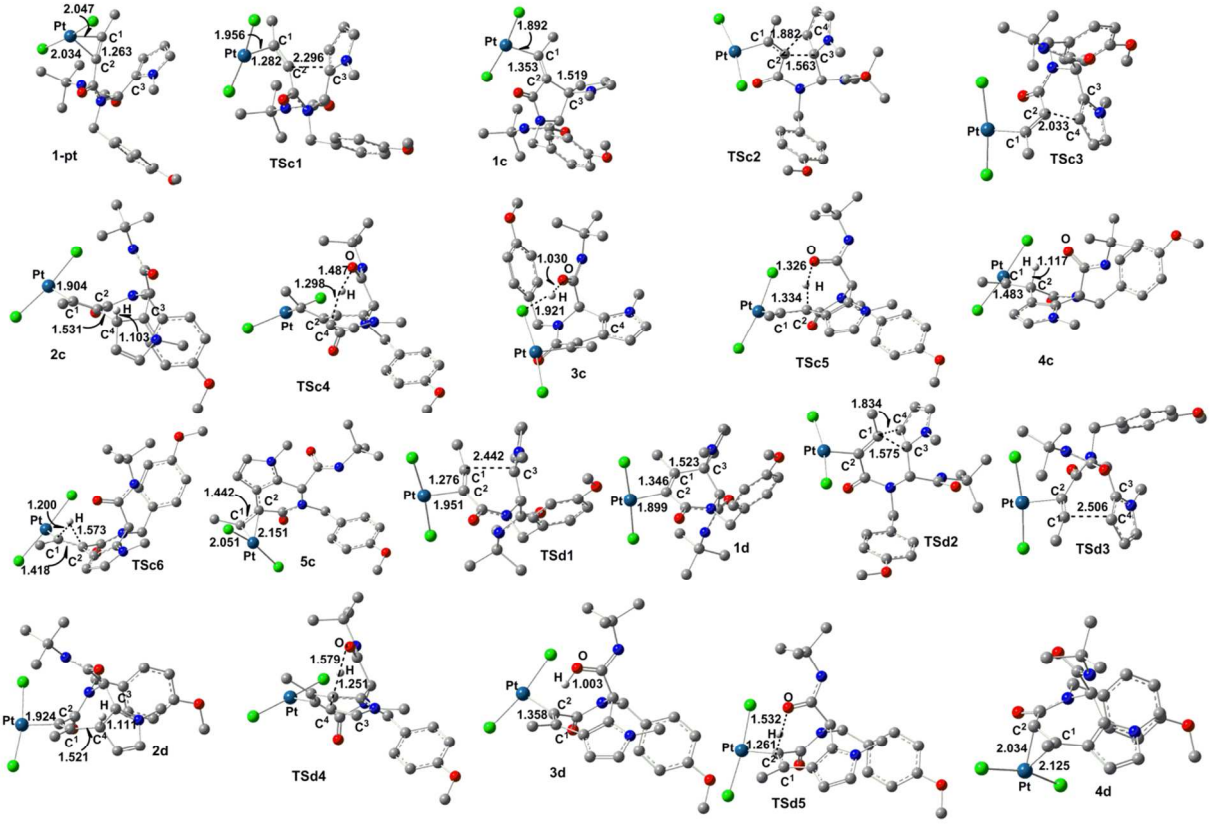

Figure 5 Optimized structures for path **c** and **d** shown in Figure 4, with selected structural parameters (bond lengths in Å).

Table 1. Thermodynamic Properties (Relative Free Energies and Activation Free Energies in Gas Phase and in Solution) of the Structures in Figure 1 and 2 [a]

System	ΔE^{rel}_{gas}	ΔG^{rel}_{gas}	$\Delta E^{\neq}_{gas}$	$\Delta G^{\neq}_{gas}$	ΔE^{rel}_{sol}	ΔG^{rel}_{sol}	$\Delta E^{\neq}_{sol}$	$\Delta G^{\neq}_{sol}$
1-Au	0	0			0	0		
TSa1	10.8	11.1	10.8	11.1	12.5	10.1	12.5	10.1
1a	-16.0	-13.7			-12.0	-12.9		
TSa2	2.3	4.9	18.3	18.6	8.5	7.0	20.5	19.9
TSa3	14.6	16.0	14.6	16.0	14.9	16.4	14.9	16.4
2a	-8.6	-6.4			-4.4	-5.1		
TSa4	-0.1	2.0	8.5	8.3	9.9	4.5	14.3	9.6
3a	-4.2	-2.0			-3.7	-6.7		

TSa5	-3.2	-1.7	0.9	0.3	6.9	1.8	10.6	8.5
4a	-35.7	-35.4			-35.3	-37.0		
TSb1	23.0	24.8	23.0	24.8	26.4	26.6	26.4	26.6
1b	-16.7	-14.2			-14.3	-14.2		
TSb2	2.5	6.3	18.5	20.0	6.9	6.6	18.9	20.8
TSb3	15.5	17.8	15.5	17.8	16.5	18.5	16.5	18.5
2b	-10.5	-7.3			-7.7	-7.0		
TSb4	-6.1	-2.3	4.4	5.0	2.1	-0.1	9.8	7.0
3b	-15.1	-12.2			-14.6	-15.0		
TSb5	-15.2	-11.7	-0.1	0.5	-6.5	-9.6	8.1	5.4
4b	-34.3	-31.7			-35.9	-34.6		

[a] These values, in kcal/mol, were calculated at the M06-2X/6-31G (d, p) (LANL2TZ(f) for Au) level of theory and included the zero-point energy correction, using single-point integral equation formalism polarizable continuum model (IEFPCM) calculations at the M06-2X/6-311++G (d, p) (LANL2TZ(f) for Au) level of theory to model the effect of the solvent .

Table 2. Thermodynamic Properties (Relative Free Energies and Activation Free Energies in Gas Phase and in Solution) of the Structures in Figure 4 and 5 [a]

System	ΔE^{rel}_{gas}	ΔG^{rel}_{gas}	$\Delta E^{\neq}_{gas}$	$\Delta G^{\neq}_{gas}$	ΔE^{rel}_{sol}	ΔG^{rel}_{sol}	$\Delta E^{\neq}_{sol}$	$\Delta G^{\neq}_{sol}$
1-Pt	0	0			0	0		
TSc1	7.5	10.3	7.5	10.3	8.3	9.2	8.3	9.2
1c	-25.1	-21.3			-34.1	-33.8		
TSc2	-13.8	-11.3	11.3	10.0	-18.0	-21.2	16.1	12.6
TSc3	7.5	9.8	7.5	9.8	7.2	10.7	7.2	10.7
2c	-18.4	-14.2			-25.8	-25.3		
TSc4	-8.1	-3.2	10.4	11.0	-9.5	-12.3	16.3	13.1

3c	-32.3	-28.3			-37.7	-41.4		
TSc5	-17.5	-15.3	14.8	13.0	-17.9	-23.8	19.8	17.5
4c	-25.5	-22.7			-26.1	-28.3		
TSc6	-12.8	-10.2	12.7	12.5	-14.2	-18.7	11.9	9.6
5c	-42.6	-39.3			-42.4	-40.4		
TSd1	8.9	12.0	8.9	12.0	8.9	10.5	8.9	10.5
1d	-26.5	-23.4			-33.9	-34.1		
TSd2	-12.4	-9.7	12.7	11.6	-15.5	-18.2	18.4	15.9
TSd3	11.6	14.6	11.6	14.6	13.4	14.1	13.4	14.1
2d	-18.5	-14.0			-24.2	-23.1		
TSd4	-15.3	-10.1	3.2	3.9	-15.7	-17.6	8.5	5.4
3d	-24.3	-20.5			-32.2	-32.9		
TSd5	-14.1	-10.2	10.2	10.3	-16.3	-20.2	15.9	12.8
4d	-41.6	-38.6			-42.7	-40.5		

[a] These values, in kcal/mol, were calculated at the M06-2X/6-31G (d, p) (LANL2TZ(f) for Pt) level of theory and included the zero-point energy correction, using single-point integral equation formalism polarizable continuum model (IEFPCM) calculations at the M06-2X/6-311++G (d, p) (LANL2TZ(f) for Pt) level of theory to model the effect of the solvent .

Graphical Abstracts

Pyrrolopyridinones and pyrroloazepinones can be prepared through gold (I) or platinum (II) catalyzed. These interesting gold (I) or platinum (II) catalyzed way is fully supported by a computational study justifying the formation of each intermediate.